COO-3077-162

Courant Mathematics and
Computing Laboratory

U.S. Department of Energy

The Application of an Explicit Numerical Method to a Reaction-Diffusion System in Combustion

Rolf D. Reitz

U.S. Department of Energy Report

Prepared under Contract EY-76-C-02-3077 with the
Office of Energy Research

Mathematics and Computing
November, 1979

New York University

UNCLASSIFIED

Courant Mathematics and Computing Laboratory

New York University

Mathematics and Computing COO-3077-162

The Application of an Explicit Numerical Method to a Reaction-Diffusion System in Combustion

Rolf D. Reitz*

*Courant Institute of Mathematical Sciences, New York University. The work of this author was supported by DOE Contract No. EY-76-C-02-3077.

U. S. Department of Energy

Contract EY-76-C-02-3077

UNCLASSIFIED

ABSTRACT

Numerical methods are applied to one-dimensional unsteady reaction-diffusion equations to seek propagating wave solutions. These equations describe flame propagation in certain combustion systems if constant pressure combustion is assumed, with Lewis number = 1 and if a Lagrangian coordinate transformation is introduced. It is shown that the steady flame speed is invariant under this coordinate transformation. Model reaction-diffusion equations which admit traveling waves as exact solutions are formulated and one of these is solved with twelve different numerical integration schemes in a test problem. The diffusion terms are differenced using the explicit methods introduced by Saul'yev, which are shown can be formally accurate to $O(\Delta t^3/\Delta x^2)$. Both implicit and explicit techniques for the reaction rate terms are tested. The results of a study with these schemes indicates that: numerical diffusion can reduce accuracy significantly, that numerical dispersion truncation errors can reduce accuracy if they are sufficiently large, and that an accurate representation of the reaction rate in the difference equations is important to retain overall accuracy. In addition to the above test problem, one of the explicit methods is applied to an ozone decomposition flame computation. An adaptive grid procedure is also implemented. The results show good agreement with the fourth order accurate results of Margolis which indicates that a more efficient lower order numerical method can be sufficiently accurate for practical computations.

LIST OF SYMBOLS

a	matching constant in Eq. (21a)
b	constant in Eq. (21a,b)
B	pre-exponential constant in Eq. (40)
c	zone specifying constant in Eq. (34)
c_p	specific heat at constant pressure
$\mathcal{D}$,d	species diffusion coefficients
E	activation energy in Eq. (40)
F	reaction rate in Eq. (17) and (23)
h, h_1, h_2	grid point spacing in Eq. (23)
h	specific enthalpy
k	reaction rate in Eq. (40).
K	number of reaction-diffusion equations in (17)
m	constant in Eq. (18)
M	number of computational points
n	running index; $n\Delta t = t$ in Eq. (23)
N	number of chemical species
p	pressure
q	$-S\Delta t/2\Delta x$ in reaction rate of Scheme X (Eq. (23))
$\mathcal{R}$	universal gas constant
r	$d\Delta t/\Delta x^2$
s	constant in reaction rate Eq. (40)
$S, \bar{S}$	wave speed in (x,t) and $(\bar{x},\bar{t})$ planes
$t, \bar{t}$	time
T	temperature

List of Symbols, continued

u	generalized dependent variable in Eq. (17), gas velocity
U	numerical approximation to u in Eq. (23)
V,W	variables in Eq. (23)
W	species molecular weight
$x,\bar{x}$	space coordinate in (x,t) and $(\bar{x},\bar{t})$ planes
Y	species mass fraction
z	non-uniform mesh spacing = Δx for equally spaced mesh.

Greek symbols

α	adiabatic flame temperature, sum of stoichiometric indices, parameter in reaction rate of Eq. (23a,b)
β,γ,δ	parameters in reaction rate of Eq. (23a,b)
Δt	numerical time-step
Δx	mesh spacing for uniform mesh
λ	thermal conductivity of mixture
Λ	eigenvalue in Eq. (31)
μ	mixture viscosity
ν	stoichiometric index in elementary reaction step
ρ	fluid density
ω	reaction rate

Subscripts

o	quantities at $x = \infty$ in Figure 1
1	quantities at $x = -\infty$ in Figure 1
i,j	running indices $1,\ldots,M$
k,ℓ,m	running indices $1,\ldots,N$
m	running index for elementary reaction steps
r	reference value

List of Symbols, continued

Superscripts

b	backward elementary reaction step
f	forward elementary reaction step
k	running index $1,\ldots,N$.
n	numerical time level $n\Delta t = t$
'	forward reaction
"	backward reaction

1. INTRODUCTION

Detailed mathematical models are now being applied to practical problems in combustion. Attention is being given to models which include comprehensive elementary chemical kinetic and turbulence mechanisms. This trend has increased the number of equations to be solved and has stimulated research in numerical methods for the conservation equations of reacting gases.

In this paper we discuss results for one-dimensional unconfined deflagration wave propagation. The problem has been formulated in such a way that the momentum and overall mass conservation equations need not be considered. This simplification focuses attention on the treatment of reaction rate and diffusion terms in the governing equations.

The presence of reaction rate terms can cause timestep restrictions in computations of combustion. Each chemical species evolves with its own characteristic time scale, and the numerical timestep may be required to be comparable to the smallest of these time scales for reasons of stability and/or accuracy. This problem has led many researchers to use implicit solution techniques in combustion calculations.

Reaction diffusion equations have also been solved following this approach. This includes methods in which a system of coupled ordinary differential equations (O.D.E.) are solved using stiff O.D.E. routines (method of lines, Bledjian [1], Margolis [2]; operator splitting, Otey and Dwyer [3]); and methods in which

block tridiagonal matrices, which result from an implicit treatment of the diffusion terms, are computed (Lund [4]).

In this work we formulate and apply an explicit method to a one-dimensional ozone decomposition flame calculation. The motivation for the use of an explicit method is the potential for increases in efficiency and accuracy. These benefits are important considerations in flame propagation problems which involve a large number of participating chemical species. The numerical method which we used for the ozone flame problem does not have the diffusional stability restriction but the numerical timestep is limited by the Lipschitz timestep constraint, which arises from the reaction rate terms. However, the results of Section 4 of the paper show that the timestep of this explicit method is nevertheless comparable to the timestep used in the implicit method of Lund [4].

We also compare the results of several other numerical schemes which use implicit methods for the evaluation of the reaction rate. In that study however, we employed a single non-linear reaction-diffusion equation (which admits exact solutions) as a model problem.

2. GOVERNING EQUATIONS

The general set of equations which describe one-dimensional flame propagation consists of the conservation and state equations for reactive flows which can be written as follows (Williams [5]).

$$\frac{\partial \rho}{\partial t} + \frac{\partial (\rho u)}{\partial x} = 0 \tag{1}$$

$$\frac{\partial (\rho u)}{\partial t} + \frac{\partial \rho u^2}{\partial x} = -\frac{\partial p}{\partial x} + \frac{\partial}{\partial x}\left(\mu \frac{\partial u}{\partial x}\right) \tag{2}$$

$$\frac{\partial (\rho h_s)}{\partial t} + \frac{\partial (\rho u h_s)}{\partial x} = \frac{\partial p}{\partial t} + \frac{\partial}{\partial x}\left(\lambda \frac{\partial T}{\partial x}\right) + \frac{\partial}{\partial x}\left(\frac{\mu}{2} \frac{\partial u^2}{\partial x}\right) + \frac{\partial}{\partial x}\left\{\rho \sum_{k=1}^{N} \mathcal{D}^{(k)} h^{(k)} \frac{\partial Y^{(k)}}{\partial x}\right\} \tag{3}$$

$$\frac{\partial \rho Y^{(k)}}{\partial t} + \frac{\partial \rho u Y^{(k)}}{\partial x} = \frac{\partial}{\partial x}\left(\rho \mathcal{D}^{(k)} \frac{\partial Y^{(k)}}{\partial x}\right) + \omega^{(k)} \quad k=1,\ldots,N \tag{4}$$

$$p = \rho \mathcal{R} T \sum_{k=1}^{N} \left\{Y^{(k)}/W^{(k)}\right\} \tag{5}$$

where

$$h_s = \sum_{k=1}^{N} Y^{(k)} h^{(k)} + u^2/2$$

$$= \sum_{k=1}^{N} Y^{(k)} \left\{\int_{T_r}^{T} c_p^{(k)} dT' + h_r^{(k)}\right\} + u^2/2 \tag{6}$$

The first four equations are the overall mass, momentum, energy and the N species conservation equations for the N chemical species having mass fractions $Y^{(k)}$, u is the mass averaged gas velocity,

h_s is the total mixture enthalpy and p, T and ρ are the gas pressure, temperature and density. In Eq. (5), the thermal equation of state, it has been assumed that the mixture behaves as a perfect gas. Here $W^{(k)}$ is the species molecular weight. Fick's law has been employed to describe species diffusion effects with species diffusion coefficients $\mathcal{D}^{(k)}$. $\omega^{(k)}$ is the mass rate of creation or depletion of species (k) , and $h_r^{(k)}$ is the heat of formation of species (k) at temperature T_r .

Thermal radiation, body forces, Soret, Dufour, and pressure gradient diffusion, and bulk viscosity effects have been assumed to be negligible.

Model Formulation

In unconfined flame propagation the combustion wave separates the unburned gases at $x = \infty$ and the burned gases at $x = -\infty$ as depicted in Figure 1. The unburned mixture has constant density ρ_o temperature T_o and species mass fractions $Y_o^{(k)}$ and velocity $u_o = 0$. In the burned gases $\rho = \rho_1$, $T = T_1$ and $Y^{(k)} = Y_1^{(k)}$. However, the quantities at $x = -\infty$ and the wave speed, S , are unknown in general and are to be computed.

The governing equations can be reduced to a set of reaction-diffusion equations if simplifying assumptions are introduced and if a coordinate transformation is made. The constant pressure assumption, $p_1 = p_o$ valid when the flame velocity is very much less than the sound speed, allows the momentum equation (2) to be dropped.

Another consistent approximation is to neglect the terms involving the kinetic energy ($\sim u^2/2$) and its derivatives in Eqs. (3) and (6) (see Williams [5]). The convective terms in (3) and (4) can be eliminated by a Lagrangian coordinate transformation from the (x,t) plane to the $(\bar{x},\bar{t})$ plane by defining $\bar{t} = t$ and

$$\frac{\partial \bar{x}}{\partial x} = \frac{\rho}{\rho_o} \tag{7a}$$

$$\frac{\partial \bar{x}}{\partial t} = -\frac{\rho}{\rho_o} u \tag{7b}$$

This transforms Eqs. (3) and (4) into

$$\frac{\partial Y^{(k)}}{\partial \bar{t}} = \frac{\partial}{\partial \bar{x}} \left(\frac{\rho}{\rho_o}\right)^2 \mathcal{D}^{(k)} \frac{\partial Y^{(k)}}{\partial \bar{x}} + \frac{\omega^{(k)}}{\rho} \tag{8}$$

$$\frac{\partial \Sigma Y^{(k)} h^{(k)}}{\partial \bar{t}} = \frac{\partial}{\partial \bar{x}} \left(\frac{\rho}{\rho_o}\right)^2 \frac{\lambda}{\rho} \frac{\partial T}{\partial \bar{x}} + \frac{\partial}{\partial \bar{x}} \left(\frac{\rho}{\rho_o}\right)^2 \Sigma \mathcal{D}^{(k)} h^{(k)} \frac{\partial Y^{(k)}}{\partial \bar{x}} \tag{9}$$

and satisfies Eq. (1) identically. Equation (9) may be rearranged using (8) and (6) (after summation over (k) and multiplication by $h_r^{(k)}$) to give

$$\frac{\partial}{\partial \bar{t}}\left[\Sigma Y^{(k)} \int_{T_r}^{T} c_p^{(k)} dT'\right] = \frac{\partial}{\partial \bar{x}}\left[\left(\frac{\rho}{\rho_o}\right)^2 \frac{\lambda}{\rho c_p} \frac{\partial}{\partial \bar{x}} \left[\Sigma Y^{(k)} \int_{T_r}^{T} c_p^{(k)} dT'\right]\right] - \frac{\Sigma h_r^{(k)} \omega^{(k)}}{\rho}$$

$$+ \frac{\partial}{\partial \bar{x}}\left[\left(\frac{\rho}{\rho_o}\right)^2 \Sigma\left(\mathcal{D}^{(k)} - \frac{\lambda}{\rho c_p}\right) \int_{T_r}^{T} c_p^{(k)} dT' \frac{\partial Y^{(k)}}{\partial \bar{x}}\right] ;$$

$$c_p = \Sigma Y^{(k)} c_p^{(k)} .$$

Finally, with the further assumptions that for all k, $c_p^{(k)} = c_p$, $\mathcal{D}^{(k)} = \mathcal{D}$ where c_p and $\mathcal{D}$ are constants, and that $\rho\mathcal{D} = \lambda/c_p$ (Lewis number = 1) we have the reaction diffusion equation system

$$\frac{\partial T}{\partial \bar{t}} = \frac{\partial}{\partial \bar{x}}\left(\frac{\rho}{\rho_o}\right)^2 \mathcal{D}\frac{\partial T}{\partial \bar{x}} - \frac{\Sigma h_r^{(k)}\omega^{(k)}}{\rho c_p} \tag{10}$$

$$\frac{\partial Y^{(k)}}{\partial \bar{t}} = \frac{\partial}{\partial \bar{x}}\left(\frac{\rho}{\rho_o}\right)^2 \mathcal{D}\frac{\partial Y^{(k)}}{\partial \bar{x}} + \frac{\omega^{(k)}}{\rho} \tag{11}$$

Supplemented by the equation of state

$$\rho T \Sigma Y^{(k)}/W^{(k)} = p/\mathcal{R} = \text{const.} \tag{12}$$

and the boundary conditions (which enforce zero diffusion of heat or mass at $\pm\infty$).

$$\left.\begin{aligned} \rho &= \rho_o \\ T &= T_o \\ Y^{(k)} &= Y_o^{(k)} \end{aligned}\right\} \quad \left.\begin{aligned} \frac{\partial Y^{(k)}}{\partial \bar{x}} &= 0 \\ \frac{\partial T}{\partial \bar{x}} &= 0 \end{aligned}\right\} \quad \text{at } \bar{x} = \infty$$

$$\left.\begin{aligned} \frac{\partial Y^{(k)}}{\partial \bar{x}} &= 0 \\ \frac{\partial T}{\partial \bar{x}} &= 0 \end{aligned}\right\} \quad \text{at } \bar{x} = -\infty \tag{13}$$

for $k = 1,\ldots,N$.

Conventionally, the gas velocity, u, and the wave speed,

S, is determined by integration of Eq. (7a,b), once Eqs. (10) to (13) have been solved. However, notice that in steady propagation the wave speed is invariant under the transformations (7a,b) This is because in steady wave propagation

$$\frac{\partial}{\partial t} + S\frac{\partial}{\partial x} = \frac{\partial}{\partial \bar{t}} + \bar{S}\frac{\partial}{\partial \bar{x}} = 0 \quad , \tag{14}$$

and therefore (4) and (8) may be integrated (subject to Eqs. (13) which are the same in both coordinate systems) to show that

$$\rho(u - S)Y^{(k)}\Big|_{-\infty}^{\infty} = \int_{-\infty}^{\infty} \omega^{(k)}\, dx \tag{15}$$

$$-\bar{S}\, Y^{(k)}\Big|_{-\infty}^{\infty} = \int_{-\infty}^{\infty} \frac{\omega^{(k)}}{\rho}\, d\bar{x} \tag{16}$$

Now equation (1) shows that $\rho(u - S) = \text{const.} = -\rho_o S$, and the use of (7a) in (15) and a comparison with (16) verifies that $S = \bar{S}$. This observation simplifies the determination of the steady state flame speed from computational results obtained in the $\bar{x},\bar{t}$ plane. In summary then, Eqs. (10), (11) and (13) are written in the generalized form

$$\frac{\partial u^{(k)}}{\partial t} = \frac{\partial}{\partial x}\left\{ d^{(k)} \frac{\partial u^{(k)}}{\partial x} \right\} + F^{(k)}\left(u^{(1)},\ldots,u^{(K)}\right)$$

subject to the boundary conditions

$$\frac{\partial u^{(k)}}{\partial x}(\infty,t) = \frac{\partial u^{(k)}}{\partial x}(-\infty,t) = 0 \; ; \quad k = 1,\ldots,K \quad . \tag{17}$$

We now consider the case $K = 1$ and $d^{(1)} = d = \text{constant}$. $u = u^{(1)}$ could be taken to represent non-dimensional temperature such that $0 \leq u \leq \alpha$, where α is the adiabatic flame temperature. This simplification of Eqs. (10) and (11) can be shown to be valid for the case of a global irreversible one-step chemical kinetic mechanism with a stoichiometrically premixed mixture of reactants.

In this case $F(u)$ (≥ 0) is usually given by a non-linear Arrhenius expression (see Eq. (40)). Spalding [6] proposed a simpler algebraic expression

$$F(u) = \beta u^n (\alpha - u)^m \; , \tag{18}$$

which approximates the Arrhenius function for large positive, n, but no exact solutions have previously been found for this model.

It is noted here that exact travelling wave solutions can be found for $n=2$ and $m=1$ or, more generally, for F given by

$$F(u) = \beta u^{m+1}(\alpha - u^m) \; , \quad m > 0 \quad . \tag{19}$$

The solutions are given by

$$u(x - St) = \left[\alpha / \left\{ 1 + e^{\frac{mS}{d}(x-St)} \right\}\right]^{1/m} \; , \tag{20}$$

and they correspond to the class of stable minimal wave speed solutions, with exponential decay for $x \to \infty$, which are discussed by Lin [16].

In Eq. (20) the wave speed is

$$S = \alpha(\beta d/m+1)^{\frac{1}{2}}$$

An additional model equation is $n = m = 1$ in Eq. (18). This problem (Fisher's Equation) has been analysed theoretically by Kolmogoroff et al. [7] and numerically by Gazdag and Canosa [8] in studies which show the existence of a minimum wave speed. McKean [9] has shown that the final steady state wave speed is determined by the nature of the initial data. In particular, for initial data which decays exponentially ahead of the wave, i.e.

$$u(x,0) = ae^{-bx} \qquad (x \to \infty) \tag{21a}$$

where a and b are constants, the asymptotic steady state wave speed is

$$S = b + 1/b \quad . \tag{21b}$$

Ablowitz and Zeppetella [10] have found, for the particular wave speed $S = 5/\sqrt{6}$, that an exact travelling wave solution of the Fisher Equation is given by (here $\alpha = \beta = d = 1$)

$$u(x - 5/\sqrt{6}\ t) = \left\{1 + e^{(x-5/\sqrt{6}\ t)/\sqrt{6}}\right\}^{-2} \quad . \tag{22}$$

3. NUMERICAL METHOD

We describe an explicit numerical method for reaction-diffusion equations which will be shown to be accurate to $O(\Delta t^3/h^2)$ under certain conditions. The method is given in Eq. (23) below. Variations of the method, and particularly several implicit treatments of the reaction rate terms, are obtained by varying the parameters γ, δ, α, q, β in the equations. Discussion of the implicit methods, $\delta \neq 0$, is however postponed until the next section. In this section we also describe an adaptive grid method which is used in the ozone flame computations to be discussed in section 4.

We consider a finite difference scheme in which the diffusion terms in Eq. (17) are differenced using the explicit method first introduced by Saul'yev [11]. He was only able to show that the numerical method was accurate to $O(\Delta t^2/\Delta x^2)$. The finite difference approximation to the continuum solution $U^n_{k,j} \simeq u^{(k)}(x_j, n\Delta t)$ is computed at grid points x_j from the set of equations

$$\frac{V_j - U^n_{k,j}}{\Delta t} = \frac{1}{h_1 h_2 h} \left\{ h_1 \left(d^n_{k,j+1} + d^n_{k,j} \right) \left(U^n_{k,j+1} - U^n_{k,j} \right) \right.$$

$$\left. - h_2 \left[\gamma \left(\overline{d^{n+1}_{k,j}} + \overline{d^{n+1}_{k,j-1}} \right) (V_j - V_{j-1}) + (1-\gamma) \left(d^n_{k,j} + d^n_{k,j-1} \right) \left(U^n_{k,j} - U^n_{k,j-1} \right) \right] \right.$$

$$+ \delta F_k(V_j) + \alpha F_k\left(U^n_{\ell,j+qh_1} \right) + \beta F_k\left(U^{n-1}_{\ell,j} \right) \quad . \qquad (23a)$$

$$\frac{W_i - U^n_{k,i}}{\Delta t} = \frac{1}{h_1 h_2' h'} \left\{ -h_2' \left(d^n_{k,i} + d^n_{k,i-1} \right) \left(U^n_{k,i} - U^n_{k,i-1} \right) \right.$$

$$\left. + h_1' \left[\gamma \left(\overline{d^{n+1}_{k,i+1}} + \overline{d^{n+1}_{k,i}} \right) \left(W_{i+1} - W_i \right) + (1-\gamma) \left(d^n_{k,i+1} + d^n_{k,i} \right) \left(U^n_{k,i+1} - U^n_{k,i} \right) \right] \right\}$$

$$+ \delta F_k(W_i) + \alpha F_k\left(U^n_{\ell, i+q h_1'} \right) + \beta F_k\left(U^{n-1}_{\ell,i} \right) \qquad (23b)$$

$$U^{n+1}_{k,j} = (V_j + W_j)/2 \qquad (23c)$$

where

$$h_1 = x_j - x_{j-1} \; ; \quad h_2 = x_{j+1} - x_j \; ; \quad h = h_1 + h_2$$

$$h_1' = x_i - x_{i-1} \; ; \quad h_2' = x_{i+1} - x_i \; ; \quad h' = h_1' + h_2'$$

$$j = 1,2,\ldots,M \; ; \quad i = M - j + 1$$

$$k = 1,2,\ldots,K \; ; \quad \ell = 1,2,\ldots,K$$

and M is the number of computational points. In the present discussion we take

$$\delta = q = 0$$

$$\alpha = 3/2 \; ; \quad \beta = -1/2 \qquad (23d)$$

In this case, Eq. (23a,b) consist of two predictor sweeps of the mesh (in opposite directions) followed by a corrector step in Eq. (23c), with the reaction terms being given by an explicit extrapolation formula. Computationally, the operation count is similar to that of the back substitution steps in the LU decomposition of the matrices in certain implicit methods.

The difference equations (23) are still implicit in the diffusion coefficients $\overline{d_{k,j}^{n+1}}$. This difficulty is avoided if it is assumed that $\overline{d_{k,j}^{n+1}} \simeq d_{k,j}^{n}$ or if $\overline{d_{k,j}^{n+1}}$ can be computed from quantities whose values are already known at time level n+1 . We will assume the latter to be the case. In addition, Eqs. (23) are also implicit in the boundary conditions, but this is not of concern in wave propagation problems due to the specification of Neumann boundary conditions as in Eqs. (13) (Roache [12]).

We now show that the numerical method represented by Eqs. (23) has leading terms, given by a formal truncation error analysis, which are similar to those of the second-order accurate Crank-Nicolson [13] method. Notice that the Crank-Nicolson method is obtained by replacing V_j and W_j by $U_{k,j}^{n+1}$ in Eqs. (23) with $\gamma = \delta = \alpha = 1/2$ and $q = \beta = 0$. In the present example we use an equally spaced mesh $h_1 = h_2 = h/2$.

Expanding terms in (23) in a Taylor series about the continuum solution $u^{(k)}(x_j,(n+1)\Delta t)$ shows that the continuum analog of the difference equations is

$$u_t - (du_x)_x - F(u) = \frac{\Delta t}{2}\left(u_t - (du_x)_x - F(u)\right)_t$$

$$- \frac{\Delta t}{2}(1-\gamma)(du_x)_{xt} - \frac{d\gamma}{h}(V-W)_x$$

$$+ O\left(\gamma h(V-W)_{xxx}, \Delta t^2, h^2, \Delta t h\right) \qquad (24)$$

where the superscript (k) has been dropped for simplicity and the subscripts t and x indicate differentiation. The second and third terms on the right hand side of Eq. (24) and the $O\left(h(V-W)_{xxx}\right)$ term (which will be seen to be $O(\Delta t^2)$), represent a departure from the first order Crank-Nicolson truncation error form. The term involving $(V-W)_x$ may be estimated by subtracting the Taylor expansion of Eq. (23b) from that of (23a) giving

$$V - W = -\frac{4\Delta t^2\gamma}{h}(du_x)_t + \frac{2\Delta t^3\gamma}{h}(du_x)_{tt} + \frac{\Delta t\gamma}{2}\left(d(V-W)_x\right)_x + H.O.T. \quad .$$

With this result, a regular perturbation analysis with small parameter Δt shows that

$$V - W = -\frac{4\Delta t^2\gamma}{n}(du_x)_t + \frac{2\Delta t^3\gamma}{h}\left((du_x)_{tt} - \gamma\left(d(du_x)_{xt}\right)_x\right) + H.O.T.$$

Substituting this equation in Eq. (24) gives

$$u_t - (du_x)_x - F(u) = \frac{\Delta t}{2}\left(u_t - (du_x)_x - F(u)\right)_t$$

$$+ \frac{\Delta t}{2}\left(2\gamma^2 r - (1-\gamma)\right)(du_x)_{xt}$$

$$- \frac{\Delta t^2\gamma^2 r}{2}\left((du_x)_{ttx} - \gamma\left(d(du_x)_{xt}\right)_{xx}\right) + H.O.T. \quad (25$$

where $r = d\Delta t/(h/2)^2$. From this result it is seen that if d = const and

$$\gamma = \frac{\sqrt{1+8r} - 1}{4r} \qquad (26)$$

the scheme is accurate to $O(\Delta t^3/h^2)$. Formal second order

accuracy only occurs, under the additional constraints $F(u) = 0$ and $\gamma = 1$ which, in view of (26) implies that $r \simeq 0$.

The condition for diffusional stability of the method in Eqs. (23) is (Saul'yev [11])

$$\frac{1}{r} \geq 2(1-\gamma) \tag{27}$$

and it is thus unconditionally stable for $\gamma \geq 1$. However, the Lipschitz time step constraint

$$\Delta t \leq \frac{\text{const}}{\max_j \left| \frac{\partial F_k(U_{\ell,j})}{\partial U_{m,j}} \right|} \tag{28}$$

is present, and recently Hoff [14] has shown that this can make an unconditionally stable scheme for the diffusion operator only conditionally stable for the combined reaction-diffusion system.

Finally, in this section we describe the variable timestep and adaptive grid procedures which were used in the ozone decomposition flame computations. The allowable timestep was found, not from Eq. (28), but rather by requiring that the species mass fractions remain positive at every computational point. If negative mass fractions were found, the timestep was halved and that computational cycle was repeated; after 20 such computational steps the timestep was doubled. A three time level explicit scheme (VIIIb in Table I) was used in those computations. Interpolation (or extrapolation) between time levels, with a change in timestep, was avoided by adjusting the parameters α and β in Eqs. (23a,b).

The parameters were changed such that the first order truncation error of the reaction term remained equal to $-\frac{\Delta t}{2} F_t$ (see Table 1; scheme VIIIb) where Δt now corresponds to the new timestep.

The adaptive grid method is similar to that used by Lund [4] but, because the mesh function is prescribed analytically, it is simpler to implement. The non-uniform mesh was generated using parameters from the solution of an associated eigenvalue problem. A new mesh was generated when changes in the numerical solution occurred beyond a prescribed tolerance, and the solution variables were interpolated onto the updated mesh. The details are as follows.

If $z(x)$ is a continuous variable which represents the mesh spacing at point x, a variational problem is formulated which minimizes the integral

$$I(z) = \int_{x_1}^{x_M} \frac{dx}{z}\left(\frac{dz}{dx}\right)^2 , \tag{29}$$

Subject to the constraint

$$M' = \int_{x_1}^{x_M} \frac{dx}{z} . \tag{30}$$

Minimizing the integral in Eq. (29) minimizes the change in mesh spacing across the domain where x_1 and x_M are fixed boundary points, while Eq. (30) conserves the number of zones $M' = M - 1$.

Equations (29) and (30) lead to the Euler equation

$$2z \frac{d^2z}{dx^2} - \left(\frac{dz}{dx}\right)^2 - \Lambda = 0 \tag{31}$$

which is to be solved subject to the boundary conditions

$$\begin{aligned} z(x_1) &= z_1 \\ z(x_M) &= z_M \end{aligned} \tag{32}$$

Equation (31) may be readily integrated to give the parabola

$$z = \frac{c_1}{4}(x + c_2)^2 + \frac{\Lambda}{c_1}$$

where the constants of integration c_1 and c_2 may be determined from (32). However, since the desired mesh spacing at the boundaries (z_1 and z_M) is not known, c_1 and c_2 were found using an alternate procedure. The position where the largest gradient of temperature $\left.\frac{\partial T}{\partial x}\right)_{max}$ occurs is denoted by x_{min}. By requiring that the value of the mesh function, z_{min}, coincides with this point, the constants c_1 and c_2 are determined, i.e.,

$$z(x) = \frac{\Lambda}{4z_{min}}(x - x_{min})^2 + z_{min} \tag{33}$$

where

$$z_{min} = c\left|\frac{\Delta T}{\left.\frac{\partial T}{\partial x}\right)_{max}}\right| \tag{34}$$

c is a specified constant which is related to the number of zones in the region of large temperature gradient, and ΔT is the difference between the maximum (T_2) and minimum (T_1) values of temperature in the domain.

The eigenvalue Λ was determined by iteration from the equation

$$\frac{M'\sqrt{\Lambda}}{2} = \text{Tan}^{-1}\left\{\frac{(x-x_{min})}{z_{min}}\frac{\sqrt{\Lambda}}{2}\right\}\Bigg|_{x=x_1}^{x=x_M} \tag{35}$$

Eq. 35 is obtained by integrating Eq. (30) with $z(x)$ given in (33) . The special case $\Lambda = 0$ corresponds to an equally spaced mesh, while $\Lambda = (2\pi/M')^2$ corresponds to the case $x_M \to \infty$, $x_1 \to -\infty$. Equation (35), with the upper limit x_M replaced by x_j and M' replaced by $j-1$ then served to define the new mesh, for $j=2,\ldots,M-1$. The mesh was redefined if the new x_{min} and z_{min} violated either of the two inequalities

$$x_{min} - z_{min} \leq x^o_{min} \leq x_{min} + z_{min}$$

$$\frac{z^o_{min}}{2} \leq z_{min} \leq 2z^o_{min}$$

where x^o_{min}, z^o_{min} defined the mesh at the previous remap.

The solution variables (e.g. the temperature T_i at x_i) were mapped onto the new mesh x_j with the non-linear interpolation formula

$$T_j = \frac{T_1 + h_j T_2}{1 + h_j} \tag{36a}$$

where

$$h_j = g_i^{1-\alpha} g_{i+1}^{\alpha}$$

$$g_i = \frac{T_i - T_1}{T_2 - T_i}$$

and $\alpha = \dfrac{x_j - x_i}{x_{i+1} - x_i}$ for $x_i \leq x_j \leq x_{i+1}$ and $T_i \neq T_1, T_2$. This interpolation is exact for the model Eq. (20) for the case $m = 1$. For $T_i = T_\ell$ $(\ell = 1,2)$ we used instead

$$T_j = T_{i+1} \left(\frac{T_\ell}{T_{i+1}} \right)^{1-\alpha} \tag{36b}$$

which is exact for exponential functions. Equations (36) were chosen in anticipation of solutions which have approximately exponential decay outside of a narrow flame zone.

Finally, mass conservation was enforced on the new mesh by adjusting the N species mass fractions at each grid point x_j such that

$$Y_j^{(k)} = \frac{\bar{Y}_j^{(k)}}{\sum_{k=1}^{N} \bar{Y}_j^{(k)}}$$

where $\bar{Y}_j^{(k)}$ is the species mass fraction obtained from the interpolation Eqs. (36). In practice, the correction was found to be of the order of the machine round-off error after

the first few mesh remap cycles, although the correction was significant for the discretized $\bar{Y}_j^{(k)}$ on the first specified mesh at $t = 0$.

4. DISCUSSION OF RESULTS

We first present the results of a parameter study of the numerical method described in Eqs. (23 a, b, and c). The parameters used are listed in Table I. The various schemes include implicit and explicit methods for the evaluation of reaction rate terms. A single non-linear reaction-diffusion model equation was used in these studies. We show later our computational results for a coupled system of reaction diffusion-equations describing the propagating ozone decomposition flame.

The Fisher Equation, chosen as a model equation, can be written in non-dimensional form as

$$u_t = du_{xx} + u(1 - u) \tag{37}$$

which yields travelling wave solutions with $0 \leq u \leq 1$. Notice that the quadratic form of the non-linear reaction rate term simplifies the computation of implicit methods ($\delta \neq 0$ in Eqs. (23a,b)) since they can be solved explicitly.

We set $d = 1$ and used an equally spaced mesh with the domain $-50 \leq x \leq 400$. This domain was found to be sufficient to eliminate boundary effects. The initial condition $U(x,0)$ was given by the exact solution Eq. (22), which is a

travelling wave with $S = 5/\sqrt{6}$ and $u(\infty,t) = 0$, $u(-\infty,t) = 1$.

In the results shown in Fig. 2, however, this initial condition was modified slightly. This figure shows the numerical solution $U(x)$, for various times up to time $t = 20$ using the standard explicit scheme VI in Table I on a fine mesh with $\Delta x = 0.25$, $\Delta t = 0.01$. The initial data was given by Eq. (22) for $U > 5\times10^{-6}$, but for $U \leq 5\times10^{-6}$ was given by Eq. (21a). The constant b in (21a) was set equal to 0.127, i.e. $b + 1/b \simeq 8$, and the constant a was fixed by matching the initial data at the change-over point. Notice that with these conditions Eq. (21b) would predict a change in the wave speed from its initial value of $5/\sqrt{6}$ to a final speed $S \simeq 8$.

The results shown in Fig. 2 indicate that the wave propagates to the right with its structure preserved up to $t \simeq 8$. This is followed by a transition period for $10 \lesssim t \lesssim 16$ where the wave profile undergoes a change. Finally, for $t \gtrsim 18$ the wave appears to settle to a new structure. The corresponding change in the wave speed is shown in curve 1 of Fig. 3 which shows speed versus time for time up to $t = 30$. The wave speed was computed from the relation

$$S = \int_{-\infty}^{\infty} u\,(1-u)\,dx \tag{38}$$

which is, however, only valid in the steady state (compare Eq. (16)). The results in Fig. 3 confirm that a new steady state, as measured by changes in the wave speed, is reached

with speed $\simeq 8$. This agrees with Eq. (21b) for $b = 0.127$. Curve 2 in Fig. 3 summarizes a different set of results which were obtained under the same conditions as those given by Curve 1, but where the initial condition was given only by Eq. (22). In this case the wave is seen to propagate with a speed which agrees well with the exact solution $S = 5/\sqrt{6}$ for the duration of the computation.

The sensitivity of the results to minor perturbations in the initial data which was seen in Figs. 2 and 3, indicates that the Fisher Equation could be an exacting test problem for numerical wave propagation studies. Accordingly, the twelve numerical schemes which are listed in Table I were compared for this problem, as will now be discussed with the help of Figs. 4 and 5. These figures are also plots of computed wave speed versus time. Here $\Delta x = 1$ and $\Delta t = 0.2$ and the initial data was specified with (22) (steady propagating wave with speed $S = 5/\sqrt{6}$). For the schemes I to VI shown in Fig. 4 the error in the computed wave speed appears to grow, at least initially, linearly with time. The results of schemes VII to XII are shown in Fig. 5; error growth is more modest so that greater accuracy is associated with most of these schemes.

Notice that the schemes in Table I also resemble several other standard schemes: implicit (Imp), Crank-Nicolson (CN) and explicit (Exp). Each of these methods may be formed from Eqs. (23a,b) by replacing V_j and W_j with $U_{k,j}^{n+1}$ in either the diffusion or reaction term or in both terms, and by making

the same choice of the parameters γ, δ, α, q and β as is shown in Table I. The schemes in Eqs. (23a, b and c) produce the same order Δt truncation errors as the corresponding Imp, CN and Exp schemes which are shown in the Table. These error terms are listed first in the truncation error column of the Table. However, Eqs. (23) generates additional terms, proportional to $r\Delta t$ and $r\Delta t^2$, which are given in the Table. In the case of the standard explicit method Eqs. (23a,b) become identical and reduce to the standard explicit scheme.

The underestimate of the steady wave speed which is seen in Fig. 4 for the standard explicit method VI (α=1, δ=γ=q=β=0) is primarily due to a first order numerical diffusion error. This is demonstrated by comparing the results of this scheme with the results of scheme XI (Fig. 5), which is identical to scheme VI, except that the physical diffusion coefficient d was increased by a factor of $1 + (S^2\Delta t/2d)$. Here $S^{(n)}$ was computed explicitly from Eq. (38) as the computation proceeded. This increase in d minimizes the numerical diffusion effect in steady wave propagation as is seen in the truncation error column of scheme XI in Table I.

A penalty which is associated with the significant improvement in the accuracy of the explicit method which is seen in Scheme XI is that the diffusional stability criterion $r \leq 1/2$ (Compare Eq. (27) for $\gamma = 0$) becomes more restrictive for higher wave speeds. For $S >> d/\Delta x$, the stability condition (27) is replaced by the C.F.L. condition $S\Delta t/\Delta x \leq 1$. However,

scheme XI is second order accurate for the case of steady wave propagation, and it is therefore of interest to compare its performance with others in Table I.

In scheme IX ($\delta=\alpha=1/2$, $\gamma=q=\beta=0$) the leading truncation error is $-\frac{\Delta t}{2} du_{xxt}$. In contrast to scheme VI this is a numerical dispersion error and not a diffusive error in steady propagation. A comparison of scheme IX (Fig. 5), with the results of scheme VI (Fig. 4) shows that this first order dispersive error does not deteriorate accuracy as much as the diffusive error. In fact, the accuracy of the method IX is seen to be comparable to that of the second order scheme XI.

The parameter γ in the diffusion terms of Eqs. (23a,b) is given by Eq. (26) in scheme XII. Here $q=\beta=0$ and $\delta=\alpha=1/2$. This optimal choice of the parameter γ results in a leading truncation error of the form $r\Delta t^2 \; L^{\gamma,\frac{1}{2}}(u)$. The terms $L^{\gamma,\delta}(u)$ in Table I are derived from a Taylor series expansion of the methods followed by an analysis similar to that which led to Eq. (25). In Fig. 5 it is seen that scheme XII performs as well as the second order accurate scheme XI. From this it would be concluded that the $r\Delta t^2 \; L^{\gamma,\delta}(u)$ truncation error terms are small. The results which correspond to schemes VIII a, b and X are also shown in Fig. 5, and they are seen to give accurate results. The three schemes have the same leading truncation error. However, differences in their respective truncation errors do occur in the higher order terms (see Table I) and the agreement in their results confirms that the effect of

these $O(r\Delta t^2)$ terms is small.

The additional term $\frac{\Delta t}{2}(F_t + SF_x)$, which vanishes in the steady state, in scheme X ($\gamma=\alpha=1$, $\delta=\beta=0$) comes from evaluating the reaction rate explicitly as $F(U^n_{j+q\Delta X})$ with $q = -S\Delta t/2\Delta x$. The reaction rate at $x_j+q\Delta x$ (here, $-1 < q < 0$) was determined by linear interpolation between the rates at x_j and x_{j-1} with $S^{(n)}$ given by Eq. (38). This method of computing the reaction rate minimizes a truncation error, $\frac{-\Delta t}{2} F_t$, which arises from the similar but less accurate scheme V ($\gamma=\alpha=1$, $\delta=q=\beta=0$). This may be seen by comparing scheme V in Fig. 4 with scheme X in Fig. 5. The reaction rate is evaluated implicitly in scheme VIIIa ($\gamma=1$, $\delta=\alpha=1/2$, $q=\beta=0$) and is computed explicitly, but with the same leading truncation error, in scheme VIIIb ($\gamma=1$, $\delta=q=0$, $\alpha = \frac{3}{2}$, $\beta = -\frac{1}{2}$). However, the methods VIIIa and VIIIb (dashed curve) are seen to produce similar results in Fig. 5.

The methods VIII a, b and X have a first order numerical dispersion error $r\Delta tu_{xxt}$. A comparison of their results with those of the previously discussed scheme IX, which has a truncation error $\frac{-\Delta t}{2} du_{xxt}$, shows a corresponding change of sign in the error in the computed wave speed.

The first order dispersive error is larger for scheme VII and is $(\frac{1}{2} + 4r)d\Delta tu_{xxt}$ ($\gamma=2$, $q=\beta=0$ and $\delta=\alpha=\frac{1}{2}$). Referring to Fig. 5, this scheme is seen to overestimate the steady wave speed significantly. Therefore, it would be concluded that largely numerical dispersion errors can deteriorate the accuracy

of a method.

The results shown in Fig. 4 also include schemes I to IV which have not yet been discussed. Scheme I gave the poorest results in the study. This scheme has $\gamma = 2$ and the reaction rate is evaluated fully implicitly (δ=1, α=β=q=0). The scheme has a dispersive error $4r\Delta t du_{xxt}$ which is greater than that of schemes VIIIa, b, X, but less than that of scheme VII. However, the method has, in addition, a numerical diffusion error $\frac{\Delta t}{2} U_{tt}$. A comparison between schemes VII, VIIIa, b and X (Fig. 5) and scheme I (Fig. 4) shows that this numerical diffusion term deteriorates the accuracy of the method greatly.

Finally, a comparison of the performance of schemes I to VI (Fig. 4) with that of the generally superior schemes VII to XII (Fig. 5) shows the importance of an accurate evaluation of the reaction rate. Schemes VII to XII have first order truncation errors $\sim\Delta t(U_{tt} - F_t)$. This form of truncation error would lead to a second order method in the absence of physical diffusion, i.e. d=0 , and it is seen to be preferable also for the case $d \neq 0$. In the following we present numerical results which were obtained using the explicit method VIIIb which satisfies this latter requirement and does not have a first order numerical diffusion truncation error.

We next present results for the ozone decomposition flame propagation problem, mentioned earlier, which has also been analysed in detail by Bledjian [1], Margolis [2] and by Hirschfelder et al. [15]. The elementary reaction mechanism involves

atomic oxygen O, molecular oxygen O_2 and ozone O_3 through the reactions

$$O_3 + M \underset{k_1^b}{\overset{k_1^f}{\rightleftharpoons}} O_2 + O + M$$

$$O + O_3 \underset{k_4^b}{\overset{k_4^f}{\rightleftharpoons}} O_2 + O_2$$

$$O_2 + M \underset{k_5^b}{\overset{k_5^f}{\rightleftharpoons}} O + O + M$$

In the above reaction steps M stands for any of the three chemical species O, O_2 and O_3 (hence there are 7 reactions) and the superscripts, f,b, refer to the forward and backward reactions.

The reaction rates in Eqs. (10) and (11) are computed from

$$\omega^{(k)} = \sum_{m=1}^{7} W^{(k)} \left(\nu''_{k,m} - \nu'_{k,m} \right) \left\{ R_m^f - R_m^b \right\} \tag{39}$$

where

$$R_m^f = k_m^f \rho^{\alpha'_m} \prod_{n=1}^{3} \left(\frac{y^{(n)}}{W^{(n)}} \right)^{\nu'_{n,m}}$$

and R_m^b is given correspondingly with f replaced by b and with the order constants α'_m replaced by α''_m and the stoichiometric coefficients $\nu'_{n,m}$ replaced by $\nu''_{n,m}$. These last two quantities are related through

$$\alpha'_m = \sum_{k=1}^{3} \nu'_{k,m} \quad ; \qquad \alpha''_m = \sum_{k=1}^{3} \nu''_{k,m}$$

The rate constants are given by the Arrhenius expression

$$k_m^f = B_m^f \, T^{s_m^f} \, e^{-E_m^f/RT} \tag{40}$$

with a corresponding expression for k_m^b . The values of the constants B_m , s_m and E_m are given in Table II.

Dimensionless governing reaction diffusion equations are as given in Eqs. (10) to (13), but with $\rho^2 \mathcal{D} = x_o^2/t_o$, $x = \rho_o \bar{x}/x_o$, $t = \bar{t}/t_o$ and $N = 3$. $y^{(1)}$, $y^{(2)}$ and $y^{(3)}$ are the mass fractions of O , O_2 and O_3 , and T, ρ, $\omega^{(k)}$ and $h_r^{(k)}$ are non-dimensionalized with T_o , ρ_o , t_o and $\rho_o T_o c_p$, respectively. t_o is a characteristic time scale chosen as 5.878×10^{-5} sec. and a length scale $x_o = 5.048 \times 10^{-6}$ g/cm^2 is also used in the nondimensionalization. The computational domain is $0 \leq x \leq 50$ and the initial data is prescribed as is shown in Table II. This initial data and nondimensionalization was also used by Margolis [2].

Numerical results for this ozone flame problem are shown in Fig. 6 using the method VIIIb of Table I. The figure shows our computed temperature and atomic mass fraction profiles in four separate graphs, each of which spans the computational domain. The graphs show results which correspond to $t=0$, 10, 20 and 30 where time increases from top to bottom in the figure.

The slope of the oblique line which connects the reference point in the temperature profile (T = 900°k) of each graph is proportional to the flame speed since the steady speed is invariant under the transformations (7a,b). The fact that the line is straight for $t \geq 10$ indicates that steady wave propagation has been reached. However, the mass fraction of atomic oxygen at $x = 0$, which is diminishing in the successive frames, is still several orders of magnitude larger than its equilibrium value. An adaptive grid was used with only the 15 computational points which are shown in each frame with $c = 4$ in Eq. (34). The initial conditions in Table II are such that the ignition process was essentially confined to $0.8 \leq x \leq 1.2$. During the computation the minimum grid spacing z_{min} changed from .07 at $t = 0$ to about .5 for $t \gtrsim 4$.

Details of the flame's early transient development and its steady state structure are shown in Figs. 7 and 8 respectively. The figures show temperature and atomic oxygen, molecular oxygen and ozone mass fraction profiles in portions of the computational domain. The solid curves show the numerical results obtained by Margolis [2], who used an equally spaced mesh ($\Delta x = 0.2$) and a fourth order accurate method of lines. A comparison of the results shows excellent agreement of the profiles in Fig. 7 at $t = 0.1$. In Fig. 8 ($t = 35$) the computed flame profiles also show good agreement, but the flame location differs. This is due to a difference in the computed steady state wave speed of the flame in the two calculations.

This difference in flame speed can be seen in Fig. 9. This figure shows how the computed steady state flame speed varied as a function of the number of grid points used in five separate computations. For the conditions of Fig. 8 (15 grid points) the computed wave speed differs from that given by Margolis [2] (dashed line in Fig. 9) by about 2%. Notice in Fig. 9 that the rate of convergence of the results with an increase in the number of grid points indicates that the present numerical method appears to be second order accurate. In these computations the constant c in Eq. (34) was varied in proportion with the total number of grid points as is indicated in the figure.

The flame speed was computed using the method which was indicated in the discussion of Fig. 6. It was found to vary by less than 1% in each of the 11, 15, 21 and 30 grid point calculations for $t \geq 10$. The average speed is given in Fig. 9 for $10 \leq t \leq 35$ and has the value $S = 49.8 \pm 0.1$ cm/s for 30 grid points.

The computer execution time (CDC 6600) is also shown in Fig. 9. It increases nearly linearly with the number of grid points. No program optimization was performed. Each flame calculation required about 7,500 computational cycles to reach $t = 35$. The time step ranged from $\Delta t = 0.0025$ in the transient to an average value of $\Delta t \gtrsim 0.005$, or $\Delta t \sim 3\mu s$ for $t \gtrsim 4$. Time step values were not given by Bledjian [1] or Margolis [2], but the values given by Lund [4], for a similar ozone model problem, are comparable; $\Delta t \gtrsim 0.007$, or $\Delta t \gtrsim 4\mu s$. In his

implicit code the timestep was controlled by specifying a maximum allowable number of iterations for convergence of the solution in each computational cycle.

The agreement between the timestep of the present explicit method with that of the implicit method of Lund [4] could imply that each of the mass fraction and temperature reaction-diffusion equations has a similar degree of stiffness for this ozone flame problem. In other flame problems, component species may be present which do not influence the energy release and/or flame speed significantly, but which do limit the timestep. In this case the use of stiffly stable methods for the reaction rate would be advantageous. An explicit, stiffly stable method for the reaction rate is currently being developed and tested for this case. In the method the reaction terms in Eqs. (23a, b) are replaced by

$$F_k^f\,(U_{\ell,j}^n) - \left(\frac{F_k^b(U_{\ell,j}^n)}{U_{k,j}^n}\right) U_{k,j}^{n+1}$$

where the superscripts f,b refer to the positive and negative contributions to the overall rate $F = F^f - F^b$ (Compare Eq. (39)).

The effect of this method is illustrated by applying it to the Fisher Equation (37) with $d = 0$ which has the exact solution

$$u(t) = 1 \Big/ \left(1 + \left(\frac{1-u_o}{u_o}\right) e^{-t}\right)$$

where u_o is $u(t = 0)$. The numerical solution to the scheme

$$\frac{u^{n+1}-u^n}{\Delta t} = u^n(1 - u^{n+1})$$

can be shown to be

$$u^n = 1 \Big/ \left[1 + \frac{1-u_o}{u_o} (1 + \Delta t)^{-n} \right]$$

where $(1 + \Delta t)^{-n}$ is a first order accurate approximation to $e^{-t} = e^{-n\Delta t}$.

5. CONCLUSIONS

The model equation parameter study in section 4 has shown that numerical diffusion effects can reduce the accuracy of a numerical method significantly. Numerical dispersion truncation errors were also found to be detrimental to accuracy, but only if they were sufficiently large. The study also points out that the reaction rate term should be accurately represented in the finite difference scheme. Generally, methods which were second order accurate for the case of no physical diffusion, $d = 0$, were found to be best.

The explicit scheme VIIIb, which was selected for the ozone flame calculations, was found to behave like a second order accurate scheme. The scheme has no first order numerical diffusion error and from the results it is concluded that the effect of the dispersive error term and the $O(\Delta t^3/h^2)$ truncation terms was minimal.

The favorable comparison of the ozone flame results with the results of the fourth order accurate method of Margolis [2] indicates that a second order method is sufficiently accurate for practical computations. Finally, the fact that the numerical timestep of the present explicit method was found to be comparable to the timestep used in the implicit method of Lund [4] indicates that explicit numerical methods could prove to be competitive in certain combustion problems.

ACKNOWLEDGEMENTS

The author would like to thank Professors S. Burstein and E. Isaacson for helpful discussions and comments. This work was supported under D.O.E. contract number EY-76-C-02-3077.

REFERENCES

1. L. BLEDJIAN, Combust. Flame 20 (1973), 5.

2. S.B. MARGOLIS, J. Comp. Phys. 27 (1978), 410.

3. G.R. OTEY and H.A. DWYER, A.I.A.A.J. 17 (1979), 606.

4. C.M. LUND, Lawrence Livermore Laboratory Preprint UCRL-52504 (1978).

5. F.A. WILLIAMS, "Combustion Theory," Addison-Wesley, Reading, Mass. (1965), 95.

6. D.B. SPALDING, Combust. Flame 1 (1957), 287.

7. A. KOLMOGOROFF, I. PETROVSKY and N. PISCOUNOFF, Bull. de l'Univ. d'Etat à Moscou (Ser. Intern) A1 (1937), 1.

8. J. GAZDAG and J. CANOSA, J. Appl. Probability 11 (1974), 445.

9. H.P. McKEAN, Comm. Pure Appl. Math. 28 (1975), 323.

10. M.J. ABLOWITZ and A. ZEPPETELLA, Dept. Mathematics and Computer Science, Clarkson College, Potsdam, N.Y. Preprint (1979).

11. V.K. SAUL'YEV, "Integration of Equations of Parabolic Type by the Method of Nets," Pergamon Press, New York (1964), 52.

12. P.J. ROACHE, "Computational Fluid Dynamics," Hermosa Publishers, Albuquerque, N.M. (1976), 95.

13. J. CRANK and P. NICOLSON, Proc. Camb. Phil. Soc. 32 (1947), 50.

14. D. HOFF, Siam J. Numer. Anal. 15 (1978), 1161.

15. J.O. HIRSCHFELDER, C.F. CURTISS and D.E. CAMPBELL, J. Phys. Chem. 57 (1953), 403.

16. S.S. LIN, Ph.D. Thesis, Dept. Math., U.C., Berkeley (1979).

FIGURE AND TABLE CAPTIONS

FIGURE 1 - Schematic Diagram of One-dimensional Flame Propagation Problem.

FIGURE 2 - Numerical Solution of Fisher's Equation with Initial Data-Equation (22) ($U > 5 \times 10^{-6}$) and Equation (21a) ($U \leq 5 \times 10^{-6}$).

FIGURE 3 - Computed Wave Speed versus Time for Fisher's Equation. Initial Data - Curve 1, Equations (22) and (21a) - Curve 2, Equation (22).

FIGURE 4 - Computed Wave Speed versus Time for Fisher's Equation. Initial Data - Equation (22). Schemes I - VI.

FIGURE 5 - Computed Wave Speed versus Time for Fisher's Equation. Initial Data - Equation (22). Schemes VII-XII.

FIGURE 6 - Profiles of Temperature □ and Atomic Oxygen Mass Fraction o in the Propagating Ozone Decomposition Flame for t = 0, 10, 20 and 30. 15 grid points, c = 4 in Equation (34).

FIGURE 7 - Profiles of Temperature □ and Atomic Oxygen o , Molecular Oxygen ⧖ , Ozone △ mass fractions for t = 0.1 . 15 grid points, c = 4 in Equation (34). — Results of Margolis [2].

FIGURE 8 - Profiles of Temperature □ and Atomic Oxygen o , Molecular Oxygen ⧖ , Ozone △ mass fractions for t = 35 . 15 grid points, c = 4 in Equation (34). — Results of Margolis [2].

FIGURE 9 - Variation of Computed Steady Wave Speed with Number of Grid Points M. c-constant in Equation (34). -- Wave Speed of Margolis [2].

TABLE I - Parameter Study of Numerical Method, Equations (23a, b and c). (Imp, CN, Exp - Analogous Implicit, Crank-Nicolson and Explicit Methods).

TABLE II - Constants and Initial Data for Ozone Decomposition Flame Studies.

TABLE I

Scheme	DIFFUSION		REACTION TERM					LEADING TRUNCATION ERROR*
	γ	Class	δ	α	q	β	Class	
I	2	Imp	1	0	0	0	Imp	$\frac{\Delta t}{2}u_{tt} + 4r\Delta t\phi - 2r\Delta t^2 L^{2,1}$
II	1	CN	1	0	0	0	Imp	$\frac{\Delta t}{2}(u_t - du_{xx})_t + r\Delta t\phi - \frac{r\Delta t^2}{2} L^{1,1}$
III	0	Exp	1	0	0	0	Imp	$\frac{\Delta t}{2}(u_t - 2du_{xx})_t$
IV	2	Imp	0	1	0	0	Exp	$\frac{\Delta t}{2}(u_t - 2F)_t + 4r\Delta t\phi - 2r\Delta t^2 L^{2,0}$
V	1	CN	0	1	0	0	Exp	$\frac{\Delta t}{2}(u_t - du_{xx} - 2F)_t + r\Delta t\phi - \frac{r\Delta t^2}{2} L^{1,0}$
VI	0	Exp	0	1	0	0	Exp	$\frac{\Delta t}{2}(u_t - 2du_{xx} - 2F)_t$
VII	2	Imp	1/2	1/2	0	0	CN	$\frac{\Delta t}{2}(u_t - F)_t + 4r\Delta t\phi - 2r\Delta t^2 L^{2,1/2}$
VIIIa	1	CN	1/2	1/2	0	0	CN	$\frac{\Delta t}{2} G_t + r\Delta t\phi - \frac{r\Delta t^2}{2} L^{\gamma,\delta}$
VIIIb			0	3/2	0	-1/2	CN	
IX	0	Exp	1/2	1/2	0	0	CN	$\frac{\Delta t}{2}(u_t - 2du_{xx} - F)_t$
X	1	CN	0	1	$-\frac{S\Delta t}{2\Delta x}$	0	Exp	$\frac{\Delta t}{2} G_t - \frac{\Delta t}{2}(F_t + SF_x) + r\Delta t\phi - \frac{r\Delta t^2}{2} L^{1,0}$
XI	0	Exp	0	1	0	0	Exp	$\Delta t\, G_t - \frac{\Delta t}{2}(u_{tt} - S^2 u_{xx})$
XII	Eq.(26)	CN	1/2	1/2	0	0	CN	$\frac{\Delta t}{2} G_t - \frac{r\Delta t^2}{2} L^{\gamma,1/2}$

*$G(u) = (u_t - du_{xx} - F)$; $\phi(u) = du_{xxt}$; $L^{\gamma,\delta}(u) = d[(u_t - \gamma du_{xx})_{tx} + 2\delta F_u u_{tx}]_x$

TABLE II

Rate Data	m=1,2,3	m=4	m=5,6,7
E_m^f(cal/mole)	2.414×10^4	6.000×10^3	1.1735×10^5
B_m^f(l/sec $^oK^{s_m^f}$)	6.760×10^6	4.580×10^6	5.710×10^6
s_m^f(-)	2.5	2.5	2.5
E_m^b(cal/mole)	0	9.921×10^4	0
B_m^b(l/sec $^oK^{s_m^b}$)	1.180×10^2	1.880×10^6	2.470×10^2
s_m^b(-)	3.5	2.5	3.5

Thermodynamic Data	k=1	k=2	k=3
$h_r^{(k)}$ (cal/mole)	5.8675×10^4	0	3.4535×10^4
$W^{(k)}$ (g/mole)	16	32	48
c_p(cal/g ^oK)	0.2524	p (atm.)	0.821
T_o (^oK)	300	ρ_o(g/cm^3)	1.201×10^{-3}
t_o(sec)	5.878×10^{-5}	x_o(g/cm^2)	5.048×10^{-6}

Initial Data $g(x) = \cos^5\left[\frac{\pi}{2}\left(\frac{x}{1.2}\right)^7\right]$	$0 \leq x \leq 1.2$	$1.2 < x \leq 50$
$Y^{(1)}(x,0)$	$5 \times 10^{-3} g(x)$	0
$Y^{(2)}(x,0)$	$(2+g(x))/3 - Y^{(1)}(x,0)$	2/3
$Y^{(3)}(x,0)$	$1 - Y^{(1)}(x,0) - Y^{(2)}(x,0)$	1/3
$T(x,0)$	$1 + 19g(x)/6$	1

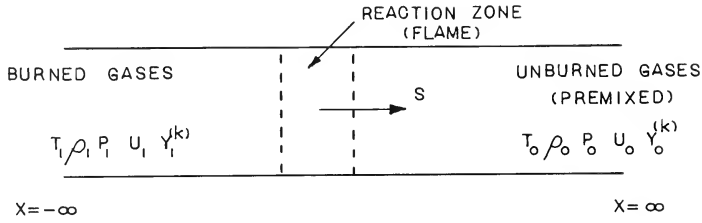
REACTION ZONE
(FLAME)
BURNED GASES
UNBURNED GASES
(PREMIXED)
S
$T_1 \rho_1 P_1 U_1 Y_1^{(k)}$
$T_o \rho_o P_o U_o Y_o^{(k)}$
$X = -\infty$
$X = \infty$

Fig. 1

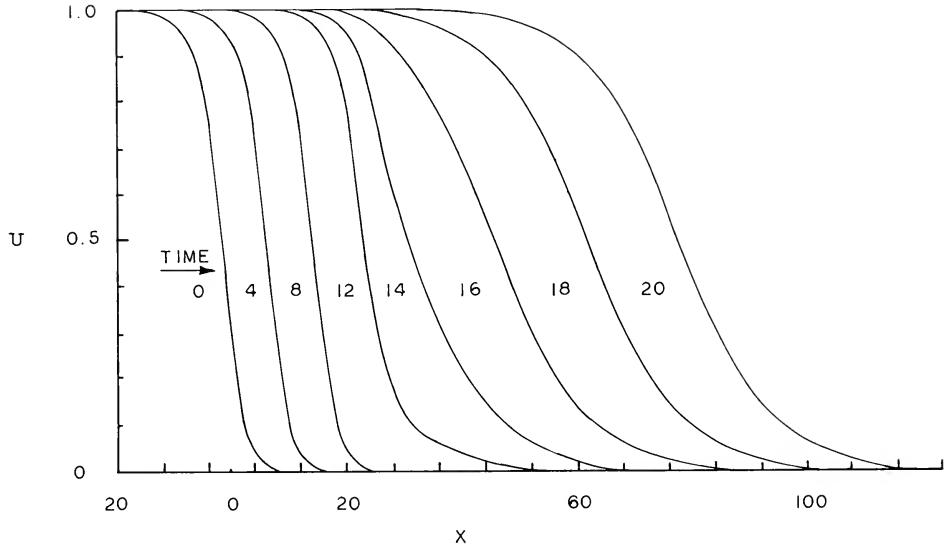

Fig. 2

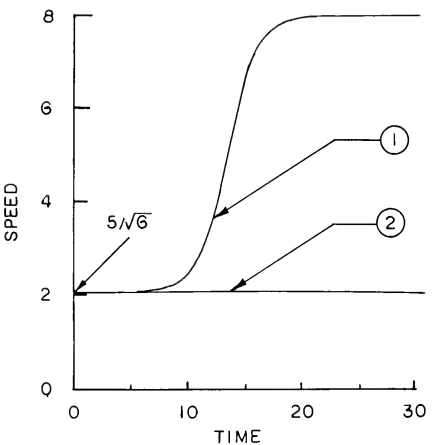

Fig. 3

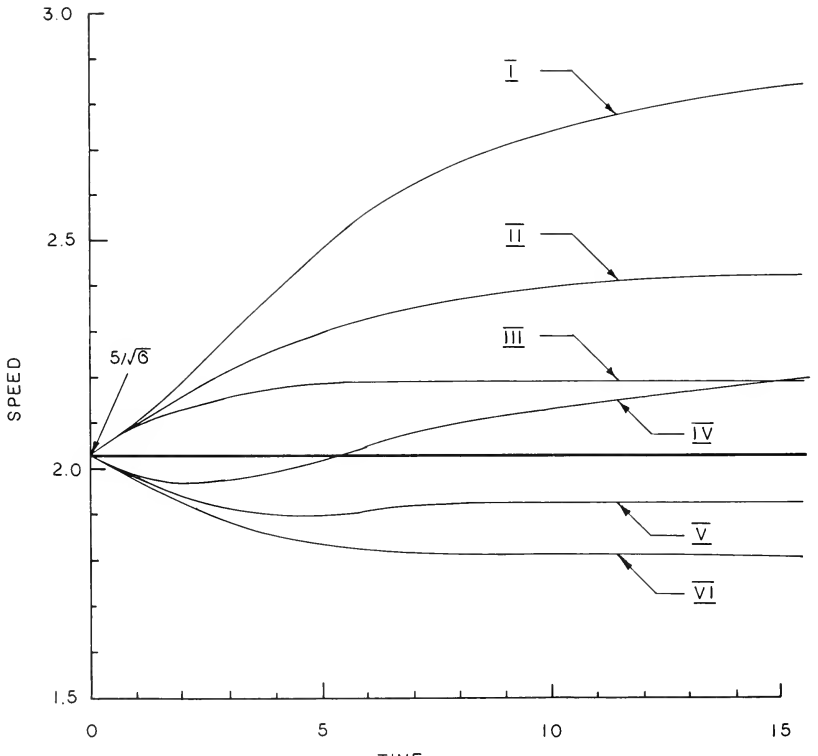

Fig. 4

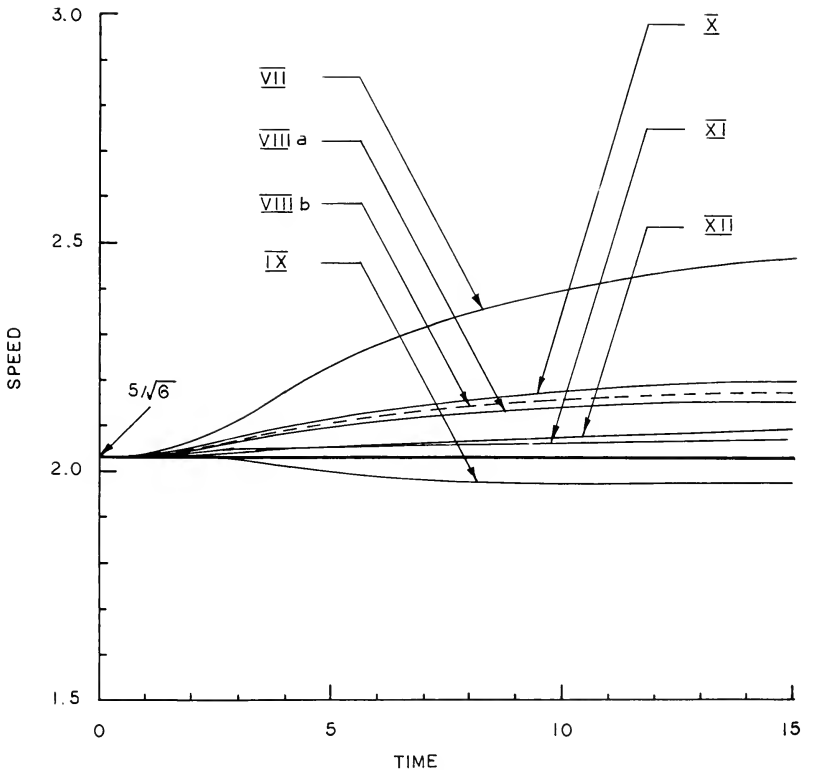

Fig. 5

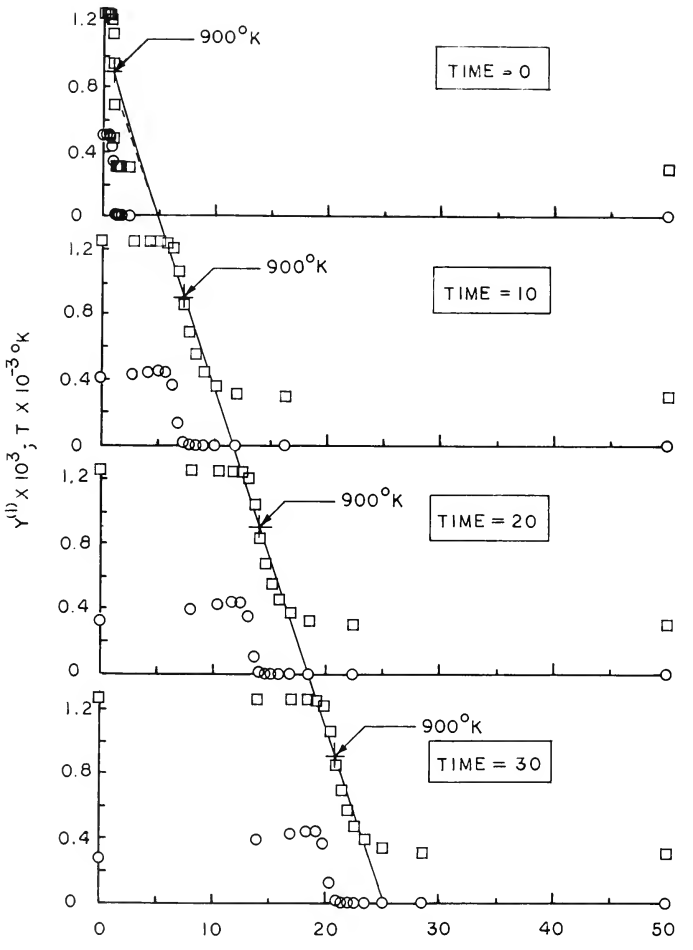
900°K
TIME = 0
900°K
TIME = 10
900°K
TIME = 20
900°K
TIME = 30
1.2
0.8
0.4
0
0
10
20
30
40
50
X
Y(1) X 10³; T X 10⁻³ °K

Fig. 6

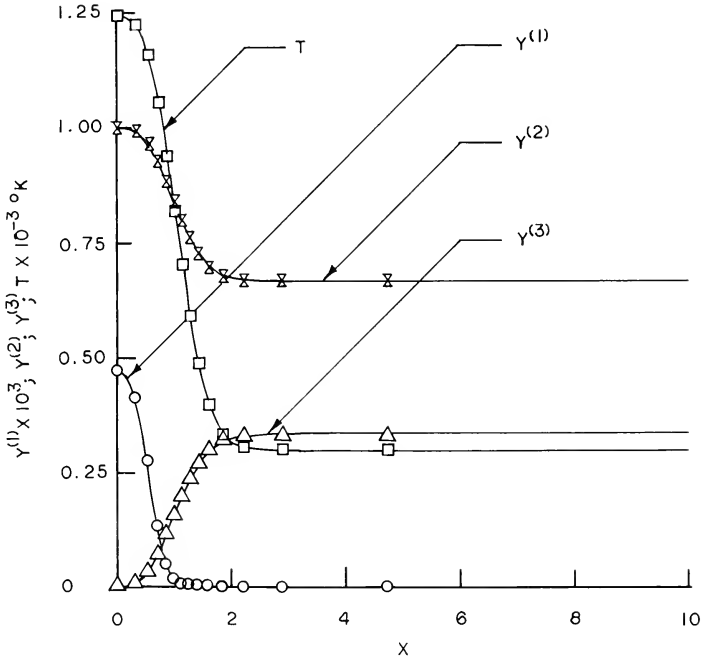
1.25
1.00
0.75
0.50
0.25
0
0
2
4
6
8
10
X
T
$Y^{(1)}$
$Y^{(2)}$
$Y^{(3)}$
$Y^{(1)} \times 10^3$; $Y^{(2)}$; $Y^{(3)}$; $T \times 10^{-3}$ °K

Fig. 7

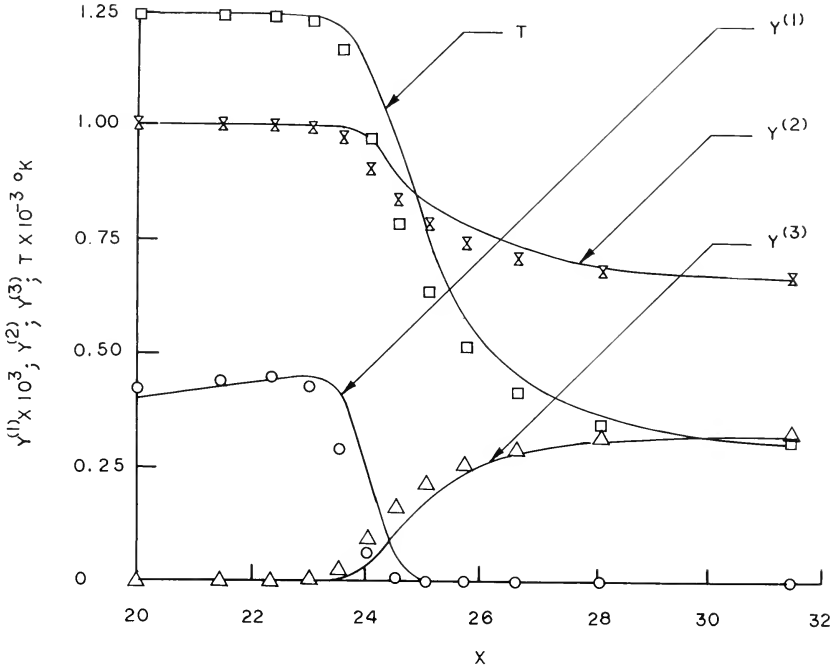
1.25
1.00
0.75
0.50
0.25
0
20
22
24
26
28
30
32
X
T
$Y^{(1)}$
$Y^{(2)}$
$Y^{(3)}$
$Y^{(1)} \times 10^3$; $Y^{(2)}$; $Y^{(3)}$; $T \times 10^{-3}$ °K

Fig. 8

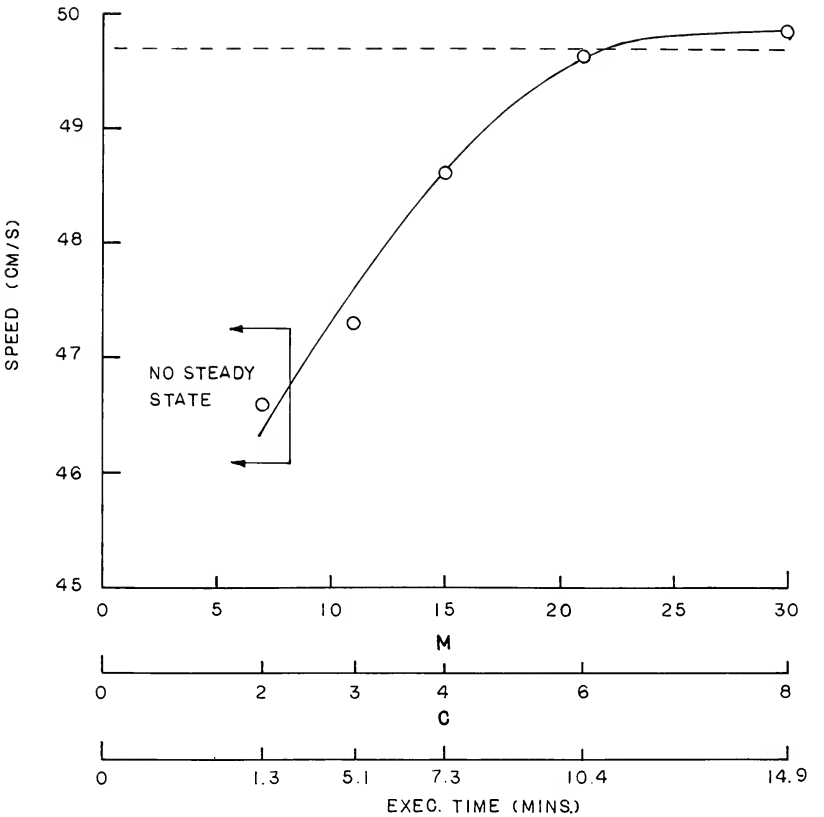
SPEED (CM/S)
50
49
48
47
46
45
NO STEADY
STATE
0
5
10
15
20
25
30
M
0
2
3
4
6
8
C
0
1.3
5.1
7.3
10.4
14.9
EXEC. TIME (MINS.)

Fig. 9

This report was prepared as an account of Government sponsored work. Neither the United States, nor the Administration, nor any person acting on behalf of the Administration:

A. Makes any warranty or representation, express or implied, with respect to the accuracy, completeness, or usefulness of the information contained in this report, or that the use of any information, apparatus, method, or process disclosed in this report may not infringe privately owned rights; or

B. Assumes any liabilities with respect to the use of, or for damages resulting from the use of any information, apparatus, method, or process disclosed in this report.

As used in the above, "person acting on behalf of the Administration" includes any employee or contractor of the Administration, or employee of such contractor, to the extent that such employee or contractor of the Administration, or employee of such contractor prepares, disseminates, or provides access to, any information pursuant to his employment or contract with the Administration, or his employment with such contractor.

This book may be kept

FOURTEEN DAYS

A fine will be charged for each day the book is kept overtime.

GAYLORD 142 PRINTED

NYU C00-3077-162 c.1
Reitz
The appl. of an explicit
numerical method to a reaction-
diffusion...

N.Y.U. Courant Institute of
Mathematical Sciences
251 Mercer St.
New York, N. Y. 10012